Photoelectron-photoion coincidence spectroscopy for multiplexed detection of intermediate species in a flame

Journal:	*Physical Chemistry Chemical Physics*
Manuscript ID:	CP-ART-06-2014-002857.R1
Article Type:	Paper
Date Submitted by the Author:	27-Aug-2014

Complete List of Authors:	Krüger, Julia; Bielefeld University, Department of Chemistry Garcia, Gustavo; Synchrotron SOLEIL, Felsmann, Daniel; Bielefeld University, Department of Chemistry Moshammer, Kai; Bielefeld University, Department of Chemistry Lackner, Alexander; Bielefeld University, Department of Chemistry Brockhinke, Andreas; Bielefeld University, Department of Chemistry Nahon, Laurent; Synchrotron SOLEIL, Kohse-Höinghaus, Katharina; Bielefeld University, Chemistry

Photoelectron-photoion coincidence spectroscopy for multiplexed detection of intermediate species in a flame

Julia Krüger[1], Gustavo A. Garcia[2], Daniel Felsmann[1], Kai Moshammer[1], Alexander Lackner[1], Andreas Brockhinke[1], Laurent Nahon[2], and Katharina Kohse-Höinghaus[1]*

[1]Department of Chemistry, Bielefeld University, Universitätsstraße 25, D-33615 Bielefeld, Germany

[2]Synchrotron SOLEIL, L'Orme des Merisiers, St Aubin, B.P. 48, 91192 Gif sur Yvette, France

*Corresponding author; Email: kkh@uni-bielefeld.de, Phone: +49 521 106-2052

Full-length article

Abstract

Complex reactive processes in the gas phase often proceed via numerous reaction steps and intermediate species that must be identified and quantified to develop an understanding of the reaction pathways and establish suitable reaction mechanisms. Here, photoelectron-photoion coincidence (PEPICO) spectroscopy has been applied to analyse combustion intermediates present in a premixed fuel-rich (ϕ=1.7) ethene-oxygen flame diluted with 25% argon, burning at a reduced pressure of 40 mbar. For the first time, multiplexing fixed-photon-energy PEPICO measurements were demonstrated in a chemically complex reactive system such as a flame in comparison with the scanning "threshold" TPEPICO approach used in recent pioneering combustion investigations. The technique presented here is capable of detecting and identifying multiple species by their cations' vibronic fingerprints, including radicals and pairs or triplets of isomers, from a single time-efficient measurement at a selected fixed photon energy. Vibrational

structures for these species have been obtained in very good agreement with scanning-mode threshold photoelectron spectra taken under the same conditions. From such spectra, the temperature in the ionisation volume was determined. Exemplary analysis of species profiles and mole fraction ratios for isomers shows favourable agreement with results obtained by more common electron ionisation and photoionisation mass spectrometry experiments. It is expected that the multiplexing fixed-photon-energy PEPICO technique can contribute effectively to the analysis of chemical reactivity and kinetics in and beyond combustion.

Keywords: Photoelectron-photoion coincidence spectroscopy, electron imaging, synchrotron radiation, ethene flame, multiplex

1. Introduction

Understanding of complex chemical reaction processes in the gas phase must often rely on accurate information regarding the compounds involved in the reaction, including their respective structure and abundance. Such involved multi-step or multi-channel reaction processes may play a role, for example, in atmospheric and photo-induced chemistry,[1–4] in combustion science,[5–8] in interstellar space[9,10] and in chemical vapour deposition.[11] To derive reaction mechanisms for these and other systems, structure-specific identification of stable and radical intermediate species is needed, and it is desirable to measure their concentrations quantitatively as a function of the relevant reaction conditions. Species measurements in such complex reaction systems, as a function of time, location, temperature, pressure or of other relevant variables must often be performed without prior in-depth knowledge of the changing composition along the reaction progress. Analytic challenges under such conditions include unambiguous detection of ideally all intermediates, in mixtures that may contain several dozens of species, with individual concentrations varying from the percent to the ppb level, in a time-economic way which ensures that physico-chemical conditions will not have changed significantly during the experiment.

Not many techniques are capable to meet these requirements. Highly sensitive and selective laser methods can be applied in different gas-phase environments to detect a number of intermediates non-invasively, and they have found widespread use, especially to measure concentrations of radicals and molecules with a small number of atoms.[11–13] For a limited number of pre-selected species, typically with large concentrations, multiplex detection of several chemical compounds at the same time is possible, for example by Raman scattering[14] and multi-sensor diode-laser[15] or multi-mode absorption spectroscopy.[16] Laser diagnostic approaches, while undoubtedly advantageous because of their ability to probe gas-phase chemistry without perturbing the system, are not of the universally applicable nature that is necessary, for example,

to probe the 40-50 most abundant intermediates simultaneously that are typically encountered even in a simplified laboratory flame. For many gas-phase reaction systems, *in situ* molecular-beam mass spectrometry (MBMS), typically using electron ionisation (EI) in its laboratory-based variants, offers the decisive advantage that basically all species, including reactive radicals, can be ionised and therefore detected, even simultaneously, by their mass-to-charge ratio.[17] This universal applicability regarding the number and nature of species probed with high sensitivity and selectivity comes at the cost of potential spectral overlaps and fragmentation, however. A highly successful development concerns MBMS instruments for gas-phase diagnostics that rely on photoionisation (PI) with synchrotron-generated tuneable vacuum ultraviolet (VUV) light.[18] These experiments use the high photon flux and very good (<50 meV) energy resolution available from such advanced light sources in the chemically interesting 6-20 eV range. They have been instrumental in providing additional structure information not available from EI-MBMS in that they have permitted isomer separation in favourable, but significant cases.[17,19–21] Combustion-related research has thus enabled further development of the synchrotron-based species detection methods such as this now-established isomer-selective PI-MBMS approach.[22]

As one of its key features, photoionisation efficiency (PIE) spectra can be obtained with VUV-PI-MBMS by scanning the photon energy with high resolution; these spectra enable, at a given mass, by comparison to databases or spectra of pure compounds, detection of isomer-specific ionisation thresholds. Especially in combustion where reaction systems can involve hundreds of elementary steps, the VUV-PI-MBMS technique has proven invaluable to newly detect previously elusive species,[21] to better understand fuel-specific reaction pathways[23] and to assess the predictive capability of reaction models.[6–8,21] Multiplexed VUV-PI-MBMS has been demonstrated in flow reactors and flames[24,25] to provide an image of the ongoing chemistry in the system under study: multiple-mass detection and scans of the photon energy can be performed

following reaction time to study the reaction progress in a slow-flow reactor[24] or as a function of height above the burner (HAB) to provide species composition profiles in premixed low-pressure flames.[25]

While the powerful capabilities of synchrotron-based photoionisation molecular-beam mass spectrometry have been widely demonstrated, especially in combustion research,[17] the technique utilises only the generated mass-resolved ion signals as a means to identify the detected species. Photoelectron-photoion coincidence (PEPICO) spectroscopy offers the potential to make use of the additional and complementary information encoded in the electron formed in the same ionisation event, and the first demonstrations of this technique in combustion-related experiments have recently been reported.[26–28] The PEPICO technique, which extracts both electrons and ions from the ionisation volume and correlates them in time, is well known and has been applied widely to spectroscopic, dynamic and thermochemical investigations.[29–32] Coupling PEPICO spectrometers to synchrotron light sources has enabled investigations with high signal intensity and high energy resolution and the use of imaging techniques.[33–35] The continuously tuneable VUV light – as in the VUV-PI-MBMS experiments mentioned before – permits access to the ionisation energies of numerous chemical species and their first excited electronic states, typically in the 6-12 eV range. Additionally some important species such as CO with an ionisation potential (IP) of 14.014 eV,[36] CO_2 (IP: 13.777 eV)[36]; H_2O (IP: 12.621 eV)[36], H_2 (IP: 15.426 eV)[36] and Ar, often used as a reference, with an IP of 15.759 eV[36] can be ionised in the range from 12-20 eV. Photoionisation for a given mass can be performed with high sensitivity and selectivity by scanning the photon energy in "threshold", *i.e.* TPEPICO experiments[37], at fixed zero kinetic energy of the electrons. Imaging schemes permit recording electron velocity maps and ion mass spectra with high efficiency, and the additional correlation of the ion position is possible with recent refinement of synchrotron-based instruments.[26,35,38] Detection of stable

and radical compounds has been demonstrated in pyrolysis[39-42] and, most recently, in flame experiments.[27,28]

In such applications, photoelectron spectra (PES) offer the benefit of much higher intrinsic selectivity than PIE spectra, because electronic states of the ion appear as distinct peaks while they are detected as changes of the slope in PIE spectra. For smaller molecules like they are discussed in this work, a decisive vibrational fingerprint can often be observed in the photoelectron spectra. Although vibrational information will be lacking in the PES of larger molecules, well-defined, structured photoelectron spectra have also been observed for combustion-relevant larger molecules as *e.g.* furan[43] and isoprene.[44] For example, such characteristic features assisted identification of the C_5H_8 isomers cyclopentene, isoprene, 1-pentyne and 1,4-pentadiene in a prepared gas mixture by their structured PES[26] that offered more information than the commonly used PIE spectra. We would thus like to remark that the electronic structure, even without the vibrational structure, constitutes a fingerprint if the photon energy is chosen high enough to reach several electronic states of the ion.

However, scanning the photon energy with meV energy resolution over a large number of species ionisation thresholds is time-consuming. PEPICO measurements at a fixed photon energy above the IPs of the species of interest, in contrast, provide the opportunity of mass-resolved multiplexed detection of species in a gas mixture with a decisive sampling time advantage. In this paper, we provide the first demonstration of fixed-energy multi-species isomer-resolved PEPICO spectroscopy in a combustion experiment with a low-pressure, flat premixed fuel-rich ethene flame as the target. The specific flame conditions have been chosen so that comparisons with previous measurements using established MBMS techniques are possible. Results from both scanning TPEPICO and fixed-photon-energy PEPICO schemes are provided. From vibrationally resolved PES spectra of the detected methyl radical, the temperature in the ionisation region has

been determined to assess the potential influence of this quantity for concentration measurements of flame intermediates. From the PEPICO experiment, species fingerprints have been obtained that are expected to provide enhanced detection reliability of isomers in complex mixtures. Such expectations have been raised as a consequence of a recent experiment performed in gas mixtures of some stable C4 and C5 compounds,[26] where the need to scan the photon energy for the analysis of many-component mixtures in a mass- and isomer-selective manner is identified as a disadvantage, shared by both PI-MBMS and threshold photoelectron spectroscopy. In the present contribution we now overcome this disadvantage by demonstrating the potential of the fixed-photon-energy PEPICO technique in the reactive, chemically complex environment of a flame for the first time.

2. Experiment

Experiments have been performed at the undulator-based DESIRS beamline[45] of the third-generation synchrotron SOLEIL using the SAPHIRS endstation equipped with the double-image spectrometer DELICIOUS III.[35] A transportable burner chamber was adapted to this endstation. DESIRS supplies finely tuneable VUV radiation in the 5-40 eV range with high flux, high spectral resolution and adjustable polarisations. A windowless gas filter filled with argon was employed to block radiation of higher harmonics from the undulator, providing a spectrally pure window of 8-15 eV for the present investigation. After passing the 6.65 m normal incidence monochromator, where a low dispersion (200 grooves/mm) grating was chosen, providing a typical bandwidth of 2-20 meV with a flux of the order of 10^{12}-10^{13} photons/sec, the VUV beam is focused into the ionisation chamber, where it is crossed at right angles with the molecular beam that is formed by extracting a gas sample from the flame. The VUV focus spot at this intersection has a diameter of roughly 100-200 μm depending on the monochromator exit slit

size. The VUV polarisation is linear in the direction parallel to the molecular beam. For normalisation of the spectra, the photon flux is recorded with a calibrated photodiode (AXUV100, IRD). A schematic of this set-up is shown in Fig. 1. In all experiments, the VUV wavelength was either kept constant or has been step-scanned in the 9-12 eV range.

A fuel-rich (ϕ=1.7) laminar premixed ethene-oxygen flame with 25% argon dilution was stabilized at 40 mbar on a homebuilt porous plug (McKenna type) burner with a diameter of 65 mm. Gas flows were regulated by calibrated mass flow controllers (MKS and Aera). The pressure was regulated by a pressure controller (MKS, 600 Series) that was connected via a throttle valve (MKS, 253B) and a manometer (MKS, Baratron 626A) to a diaphragm pump. Gas flows and flame conditions are presented in Table 1.

Samples from the flame were extracted with a quartz nozzle with 500 μm aperture diameter that was mounted on a water-cooled flange. The burner could be translated with a stepper motor to sample at different heights above the burner. Flame gases were continuously expanded into a first-stage chamber evacuated to ~10^{-3} mbar by turbomolecular pumps. The pressure difference between the burner chamber and first pumping stage supports the formation of a molecular beam, the central part of which is cut off by a copper skimmer and further expanded into the ionisation chamber at ~10^{-6} mbar. The distance between the skimmer and nozzle apertures is ~1 cm. In the ionisation chamber, the molecular beam is crossed with the ionising VUV radiation. The distance between the VUV beam and the skimmer aperture is about 55 cm.

The double-imaging PEPICO spectrometer DELICIOUS III recorded in coincidence the electrons and ions generated by the photoionisation of the molecules present in the sampled flame. While the electrons were detected via a velocity map imaging spectrometer (VMI), the cations were recorded by a Wiley-McLaren time-of-flight ion imaging analyser (WM-TOF). The

set-up is evident from the schematic in Fig. 1. Upon ionisation of a molecule from the flame gas sample by the VUV beam, the resulting photoelectron is almost instantly detected by the VMI detector due to a continuous electric field applied to the ionisation region. The set-up uses a multi-start/multi-stop analysis for electron and ion detection, where the electrons serve as time zero for coincidence events. The PEPICO spectrometer set-up, image inversion and data analysis have been described in detail in the literature.[34,35,46]

The combination of the TPEPICO approach – with scanning the photon energy across the IPs of the species under investigation – and the fixed-energy PEPICO mode of operation were applied and compared here in a flame experiment.

3. Results and discussion

As a proof of principle, we will show the methodology of using PEPICO at a fixed energy for the separation of isomers in a flame. The operation modes and the resulting spectra will be discussed first, followed by a comparison of information from spectra generated with VUV-PI-MBMS and TPEPICO. Sensitive multiplex spectra with the time-economic fixed-energy-photon PEPICO approach will then be demonstrated to provide isomer-separating capacity in a flame. Next, temperature will be determined from the analysis of flame radical PE spectra. Finally, an exemplary flame species profile evaluation will be presented in comparison with EI-MBMS and VUV-PI-MBMS results.

3.1 PEPICO and TPEPICO spectra in a flame

A visualisation of the multidimensional spatio-temporal data provided by the DELICIOUS III spectrometer is displayed in Fig. 2 for the investigated ϕ=1.7 ethene-oxygen-argon flame at a sampling height of 4 mm, a position determined to be in the flame zone where most intermediate

species are found. All coincidence events between ions and electrons are registered so that simultaneous detection of all species present in the intersection of the molecular beam with the photoionising VUV radiation is possible. Figure 2a (lower trace marked as "unfiltered") shows the raw time-of-flight spectrum for the ions detected at the fixed photon energy 10.2 eV. The raw ion and electron images are given in Fig. 2b and c, respectively. The raw total ion image of Fig. 2b deserves a comment: Due to the large distance between the last skimmer and the photon beam and the mild expansion conditions, the length of the cylindrical interaction region, equivalent to the molecular dimension along the photon axis, is very large. This long cylindrical volume, which manifests itself as a visible elongation along the north/south direction of the photoion image shown in Fig. 2b, would lead to a degradation of the mass and particle energy resolution due to severe off-axis effects in the inhomogeneous field of the extraction region. Therefore, all the data shown hereafter have been filtered in ion position so that only the ionisation events correlated to the central region of the ion image have been included into the treatment, which essentially amounts to a virtual skimming of the molecular beam. This filtering appears here to be a major advantage of the ion imaging capability of DELICIOUS III, without which the quality of the data would prevent any quantitative information to be retrieved. The advantages of this approach are readily observed in the comparison of Fig. 2c and 2d, the latter corresponding to the filtering of the raw electron image of Fig. 2c by taking into account only the coincident ions located in the region of interest (ROI) delineated in Fig. 2b. A time-of-flight spectrum for the ions detected at the fixed photon energy of 10.2 eV, filtered with respect to the ROI, with several mass/charge (*m/z*) ratios of interest marked, is included as the upper ("filtered") curve in Fig. 2a.

The spectrometer can be set to record electron and ion images and mass spectra as a function of the photon energy, which allows, among other things, to obtain the mass-filtered photoelectron spectra as a function of the photon energy, the so-called photoionisation (PI) matrix. In Fig. 3

(top) a mass-selected PI matrix for *m/z*=15 is presented for the acquisition in which the photon energy has been scanned between 9-12 eV with 3.5 meV steps and an acquisition time of 120 seconds per step. The PI matrix carries a wealth of information that can be reduced in many ways. For instance, by integrating this PI matrix from 0 to 0.015 eV electron kinetic energy (Ele KE), the threshold photoelectron spectrum (TPES) in Fig. 3 (bottom) is obtained. In this TPE spectrum, only detected photoelectrons with near zero kinetic energy are displayed against the photon energy, revealing finer structures corresponding to the excitation of particular ionic states in different levels of vibrational excitation. The integration of the PI matrix over the complete electron kinetic energy range provides the total electron yield as a function of the photon energy. Because every detected electron corresponds to a detected ion in the mass spectrum, this integration result corresponds also to the total ion yield (TIY) that is obtained in PI-MBMS experiments. The resulting TIY from integration of the image of the PI matrix in Fig. 3 (top) is included in Fig. 3 (bottom). It is immediately evident that the TPES spectrum with its much more distinct and sharp features is highly advantageous for species identification; a fact that has already been highlighted before, also in combustion-related studies[26–28] as well as in biomimetic molecular spectroscopy studies.[47]

Due to energy conservation, the information carried on a single column of the PI matrix, *i.e.* the PES at a fixed photon energy hν corresponding to that particular column, should be equivalent to the TPES from threshold up to hν. In practice, however, the dependence of the partial cross sections and the resolution on the particle's kinetic energy gives way to clear differences. In order to compare the scan and fixed-photon-energy approaches and to better understand the time/resolution compromise, we have also recorded mass-filtered photoelectron spectra at fixed photon energies. As an example, the mass-selected velocity map image for *m/z*=15 observed in the ethene-oxygen flame at HAB=4 mm is shown in Fig. 4; the 2D image is

split with the left side displaying the raw data. In order to recover the actual velocity distribution, the raw VMI data were inverted by applying the pBasex inversion algorithm[46] that performs an inverse Abel transformation to reconstruct, from the two-dimensional projection measured upon photoionisation, a 2D cut in the original three-dimensional Newton sphere of the expanding charged particles. After this inversion, concentric rings are obtained for the selected kinetic energy range of the photoelectrons that correspond to the various states of the cation, here vibrational progressions of the electronic ground state of CH_3^+. The right half in the 2D image of Fig. 4 consequently presents the mass-selected PES for detection of *m/z*=15 – which corresponds to the methyl radical – and contains similar information as the TPES, as mentioned above. The corresponding photoelectron spectrum is shown on the right side of Fig. 4. However, the overall measurement time is reduced by a factor of 30 as the measurement is performed at a single wavelength, eliminating the need of a time-consuming photon energy scan. A more detailed analysis of the merits of this approach will be given below.

3.2 Comparison of VUV-PI-MBMS, TPEPICO and PEPICO

With the aim to use the combined information that can be obtained from mass-selective detection of ions and electrons resulting from the same ionisation event in chemically complex environments such as flames, it must be ascertained that the recorded TPEPICO spectra provide indeed an unambiguous fingerprint for the detected compound under such conditions. For intermediates typically detected in flames, the methyl radical with mass 15 is one of the simplest chemical species. No interferences from other species are expected at this mass, and we have thus chosen the analysis of the information at *m/z*=15 for a first comparison with results that can be obtained in the typical VUV-PI-MBMS flame experiments. Methyl radicals, present in a mole fraction of the order of 10^{-3} in fuel-rich low-pressure hydrocarbon flames,[48,49] can be detected

sensitively in the present experiment. Radical detection in flames using TPEPICO has also been demonstrated recently by Oßwald et al..[27] They have compared measured TPES with literature photoelectron spectra and contrasted the results with the PIE curve, with somewhat noisier TPES, however.[27]

In Fig. 3, we have already compared the TPES and total ion yield determined in this work for *m/z*=15; for reference, we have included the absolute photoionisation cross section for the methyl radical from Savee et al..[50] Both TIY and cross section curves are in very good agreement although the S/N from this work is higher. The steep slope at 9.84 eV excellently agrees with the photon energy given in the TPES of the methyl radical by Cunha de Miranda et al..[51] The multiplex time-resolved photoionisation mass spectrometer of Savee et al.[50] provided an energy resolution of 0.013 eV and an interval of 0.025 eV in the photon energy scan. The set-up used here would be capable of much higher spectral resolution (sub-meV) with meV absolute energy accuracy, allowing for resolution of finer details. The real advantage of such higher resolution will come into play when multiple species at the same mass and similar ionisation energy must be distinguished.

For isomer pairs such as allene and propyne at *m/z*=40,[28] acetone and propanal at *m/z*=58,[27] acetaldehyde and ethenol at *m/z*=44[27,28] as well as for species with the same nominal mass such as ketene and propene at m/*z*=42,[28] recent TPEPICO results demonstrate promising separation capability for these species that are typically found in flames in the 10^{-3}-10^{-4} mole fraction range. Here, we compare the literature photoionisation cross sections from Cool et al.[52] for allene and propyne to the total ion yield determined in this work as shown in Fig. 5. The ionisation energies for allene of 9.691±0.003 eV[53] and propyne of 10.37±0.01 eV[54] have been determined from photoionisation and photoelectron spectra, respectively. The total ion yield in Fig. 5 exhibits two distinct parts with different slopes marking the ionisation of allene and propyne. With the relative

amounts of the two isomers in the mixture, determined further below, the complete TIY curve can be very well represented as evident from the weighted sum of the cross sections included in Fig. 5. Besides the onsets positions, not much information is provided by this TIY curve.

However, the information from the correlated electron analysis provides additional spectroscopic detail, both in scanning and fixed photon energy modes. A comparison of the TPES (obtained in scanning mode) and the PES (at fixed photon energy) for *m/z*=15 is given in Fig. 6 which includes a reference spectrum for CH_3 from the literature.[51] The vibrational fine structure in the CH_3 photoelectron signal is clearly visible from the photon energy scan. The spectra exhibit a pronounced peak, attributed to the 0-0 band origin centred around the IP of CH_3 at 9.84 eV[51] as well as further vibrational structure, which can be attributed to a vibrational progression of the ν_2 umbrella bending mode in the $CH_3\left(\tilde{X}^2A_2''\right) \rightarrow {CH_3}^+\left(\tilde{X}^1A_1'\right)$ photoionisation process.[51] Both TPES and PES from the flame are in very good agreement with each other and show structure similar to the literature spectrum which was taken in a flash pyrolysis experiment for which a vibrational temperature of 550 K was derived.[51] The full width at half maximum of the signals in the TPES is 0.03 eV, which is a factor of two better than that observed in the PES. The photon energy scan taken to record the complete TPES shown in Fig. 6 took about 30 hours, while the acquisition time of 60 minutes for the PES taken at a fixed photon energy of 10.2 eV was comparatively much shorter. Even though the PES cannot achieve in general the high spectral resolution obtained in the photon energy scans, ionisation potential and spectral signature (electronic and vibrational) of a species can be readily determined. Recording a PES at an appropriate fixed photon energy can be sufficient for unambiguous species identification in a much shorter time frame than required for scanning methods like TPEPICO and VUV-PI-MBMS.

While this flame PES measurement advantage was successfully demonstrated for the methyl radical, it is obvious that isomer mixtures will present a more challenging situation for a proof of principle. We have therefore chosen the example of allene and propyne at *m/z*=40 that has been reported in the study of Oßwald et al..[27] Figure 7 presents the TPES obtained in this work in the 9-12 eV photon energy region. The data is compared to literature PES for allene[55] and propyne[56] which show the vibrational fingerprints of both species, leading to a clear identification. The X^2E ground state of allene is well resolved in this scan. Oßwald et al.[27] have successfully demonstrated separation of these two isomers in the first investigation of a flame with the TPEPICO approach, albeit with a lower energy resolution than that obtained here.

In the PEPICO mode of operation with the DELICIOUS III spectrometer, using a fixed photon energy above the IPs of both isomers, the resulting PES also shows the vibrational spectra of allene and propyne, and it is interesting to compare these results with the TPES of Fig. 7. Two PES are reported in Fig. 8; the left panel shows the spectrum taken with a photon energy of 10.4 eV which permits photoionisation of both isomers, and the right panel provides the PES recorded at 10.2 eV which is above the IP for allene but below that of propyne. The PES at 10.4 eV shows the signatures of both cation species, comparable to the TPES recorded with a higher spectral resolution. At 10.2 eV, the resulting PES shows only the fingerprint of the allene cation, compared to a literature PES[55] which is found to be in excellent agreement. It is obvious that the vibrational structure can be resolved and that a single, time-economic measurement at a fixed, well-chosen photon energy is sufficient for a successful identification of the two isomers. Note that the spectral resolution in the fixed-photon-energy PES for allene in the right panel of Fig. 8 is comparable to that of the TPE spectrum reported by Oßwald et al.[27] that was taken in the scanning approach.

The multiplexing advantage of the PES is even more obvious for molecular masses at which more than two isomers can be present in the flame. For *m/z*=54, four stable isomers can potentially be expected as build-up products; they are listed with their corresponding IPs in Table 2. Several C_4H_8 isomers have been detected in the 10^{-3} mole fraction range in detailed speciation VUV-PI-MBMS experiments in flames. For example, Hansen et al.[60] have presented C_4H_8 PIE spectra measured in a fuel-rich cyclopentene flame, with 1,3-butadiene identified as the dominant isomer, together with 1-butyne as the second. A weighted sum of both contributions could successfully represent the measured flame PIE spectrum and allowed to conclude that 2-butyne and 1,2-butadiene were not present within the detection limit in their flame environment. Three C_4H_8 isomers, namely 1,3-butadiene, 1-butyne and 2-butyne, have been identified in different amounts by Oßwald et al.[61] in low-pressure flames of the four different butanol fuels, again with mole fractions of the order of 10^{-3}. These three isomers were also detected in the fuel-rich ethene flame studied in the present experiment. Figure 9 shows the recorded TPES for *m/z*=54 in the photon energy range from 9-12 eV and a comparison with the literature photoelectron spectra.[56,62,63] It indicates unambiguous identification via very good agreement with the IPs of these species (Table 2). Also, the characteristic fingerprints of the cations of these three structural isomers are obvious in Fig. 9. Excellent general agreement of the measured TPES with the reference spectra is seen, and numerous vibrational transitions can be observed for each isomer.

Again, the TPES (obtained in scanning mode) is compared to a PES recorded at fixed photon energy of 10.2 eV, and the results are given in Fig. 10. At this photon energy, all observed isomers for *m/z*=54 are ionised as evident from the PES, and the vibrational fingerprint regions for 1,3-butadiene and 2-butyne are clearly detected. Only for 1-butyne the cut-off is very close to its IP of 10.18 eV and thus the fingerprint with the different vibrational transitions (as in Fig. 9)

has not been recorded with the selected fixed photon energy of 10.2 eV. In addition, because of the density of neutral states close to the threshold region, the 1-butyne vertical transition at 10.18 eV might be resonantly enhanced in the PES curve. The multiplexing PES at fixed photon energy, filtered for *m/z*=54, contains remarkably detailed spectral information, well suited to identify isomeric species in a complex reactive environment. Note that *the same* fixed-photon-energy PEPICO measurement at 10.2 eV, whose raw data is displayed in Fig. 2, was used to extract the CH_3 photoelectron image (see Fig. 4) and photoelectron spectrum (see in Fig. 6) and the allene PES in Fig. 8 (right), by selecting different masses for the respective data evaluation. The multiplexing approach demonstrated here thus provides the advantage that *a single measurement* with appropriate photon energy can unambiguously identify numerous species without prior information on the flame composition. This advantageous performance is achieved even with rather limited mass resolution for the ion detection, the reason being the superior information provided by the coincident electrons.

For the selection of the respective fixed photon energy, several factors should be considered. With high photon energy, many species can be ionised simultaneously, but if the photon energy becomes too high, fragmentation can occur. Depending on the scientific question and analytic environment, energies should be optimised regarding minimum fragmentation and significant multiplexing, *i.e.* simultaneous detection of several species. In practice, different fixed photon energies must thus be chosen depending on the system and species of interest.

It is illustrative to compare the TPES and PES measured here with the derivatives of ionisation cross sections from the literature, assembled for the detection of combustion intermediate species with VUV-PI-MBMS. For example, Wang et al.[57] and Yang et al.[64] have used the flame spectrometer at the Advanced Light Source in Berkeley that has a nominal resolution of 40 meV to measure absolute cross sections for a large number of hydrocarbon species. We have

demonstrated in Fig. 3 that an ionisation cross section curve corresponds quite well with the total ion yield obtained from the integration of the PI matrix in Fig. 3. We now pursue the opposite approach in differentiating such measured cross section data from the literature as depicted in Fig. 11. The left panel shows a comparison of the measured TPES for 1,3-butadiene with the derivative of the cross section reported by Yang et al.[64] (all values given in their cross section curve in this energy range are included here; note that the photon energy intervals in their measurement did not correspond to their maximum available resolution of 40 meV). For reference, we have also included the literature photoelectron spectrum for 1,3-butadiene provided already in Fig. 9.[62] In the right panel, similar information is given for 2-butyne. Here, our measured PES at 10.2 eV is included, again showing about a factor of two lower resolution than the TPES, but still with resolved vibrational structure. Again, the PES of Carlier et al.,[56] already provided in Fig. 9, is included for comparison. Note that while the resolution of our measured TPES and the reference spectrum in the literature is similar, the set-up here would allow for scanning with <1 meV resolution, at the expense of additional measurement time, however. Also shown is the derivative of the ionisation cross section measurement for 2-butyne by Wang et al.[57], using all their reported values in the given photon energy range. This comparison shows clearly that with the regularly used step sizes and spectral resolution of the photon energy in ionisation cross section measurements, the characteristic fingerprint of an ionised species, useful for its identification, is not observed.

3.3 Temperature in the molecular beam and species profiles

From the recorded threshold photoelectron spectra and their rovibrational structure, it is possible to estimate the temperature for the species in the ionisation region. Figure 12 illustrates this approach for the methyl radical. The two stick spectra in Fig. 12, including that of Cunha de

Miranda et al.[51] exhibit somewhat different intensity distributions corresponding to different temperatures. In the work of Cunha de Miranda et al.,[51] the methyl radical was produced by flash pyrolysis, leading to a reported vibrational temperature of 550 K. In their work, the vibrational temperature was determined by calculating the intensity ratio between the main peak at 9.84 eV and the following peak at about 9.93 eV which corresponds mainly to the 2_0^0 and 2_1^1 transitions. Note that this high vibrational temperature is also responsible for the hot band that can be seen on the red side of the 0-0 band origin.

A stick spectrum was calculated here for the methyl radical by using spectroscopic constants and Franck-Condon factors from the literature[51] and the temperature-dependent Boltzmann fraction exp[-(E_{init} / k_B T_{vib})], following the procedure of Ref. 51; here, E_{init} corresponds to the energies of the initial states in the neutral CH_3 radical, k_B is the Boltzmann constant and T_{vib} the vibrational temperature corresponding to the initial state population. Comparison of the calculated spectrum with the measurements in Fig. 12 yields an estimated temperature of 280 K for the methyl radical in the ionisation region in the molecular beam. This value is much lower than the flame temperature, which is of the order of 1700 K at the sampling location at HAB=4 mm, due to adiabatic cooling in the expansion stage. Similar results have been observed by Kamphus et al.[65] in a propene-oxygen flame, who have analysed the temperature of the molecular beam in the ionisation volume with resonance-enhanced multi-photon ionisation (REMPI) of NO and benzene. In their study, temperatures in the ionisation volume between 300 K and 450 K were determined, depending on the measurement procedure, the sampled distance from the burner, the used quartz sampling nozzle and the overall flame conditions. With respect to these influence parameters, a temperature of 280 K determined here seems very reasonable. From the methyl case we can state that besides the chemical reaction analysis interest, a flame is a powerful source of "lukewarm" high-density radicals, very well suited for

spectroscopic analysis, and definitely competitive as compared with the widely used flash pyrolysis method, to the expense of a more cumbersome set-up.

To unravel and understand a chemical reaction mechanism, it is not only instructive to identify the chemical species involved in the reaction, but their quantitative concentrations should be determined along the reaction pathway. An important fraction of the current knowledge about the combustion chemistry for relevant fuels and fuel mixtures has been derived from measurements of absolute mole fraction profiles for a large number of species, generated for example in flat premixed flames like that in the present study. Such information is important to examine dominant reaction pathways, for example regarding pollutant formation, and to develop and validate numerical models of the process. Quantitative isomer-specific species profiles as a function of height above the burner are typically reported from VUV-PI-MBMS investigations. It remains a challenge to provide similarly detailed sets of quantitative species profiles from the TPEPICO/PEPICO approaches newly adopted for combustion studies.

In their recent study, Oßwald et al.[27] have demonstrated that quantitative major species mole fraction profiles in a flame (fuel and oxygen as well as CO, CO_2, H_2O and H_2 as products of incomplete combustion under fuel-rich conditions) can be obtained using the same strategies as applied for PI-MBMS measurements, although the authors have realised that TPEPICO signal proportionalities may deviate from those measured with PI-MBMS experiments. Their results for a fuel-rich ethene-oxygen flame are in very good agreement with a simulation using the model by Taatjes et al..[66] Intermediate species mole fractions have also been given in their work[27] and in Ref. 28, based upon TPEPICO spectra taken at the Swiss Light Source. The procedure for quantitative intermediate species mole fraction evaluation, detailed in Ref. 27, has been modified from the routines of PI-MBMS evaluation to take specific parameters of their set-up, including the limited energy range of the used electron imaging detector, into account. It has, however, not

been demonstrated before that multiplexed, fixed-photon-energy PEPICO measurements can be used to derive mole fraction profile sets from a flame.

In a first illustrative example, we have here performed measurements for different heights at constant photon energy of 10.4 eV. All other parameters including acquisition time and monochromator slit size have been kept constant for the detection of the photoelectron spectra. With the results presented for this energy, determination of absolute mole fractions is not possible since the profile for argon as an internal calibration standard was not recorded – to permit detection of Ar with an IP of 15.759,[36] the gas composition in the gas filter would have had to be changed. It is, however, possible to determine relative concentration profiles as a function of the height above burner and to determine ratios of isomers. These results can be compared with absolute mole fractions determined for very similar flame conditions as reported by Felsmann et al.,[28] performed with VUV-PI-MBMS at the Advanced Light Source in Berkeley and with EI-MBMS in Bielefeld.[67]

Figure 13 shows the relative mole fraction profiles for the methyl radical (*m/z*=15) and for propyne (*m/z*=40), derived from integration of the PES over the respective vibrational structures after normalisation by the counts detected for the electron at the respective mass. For methyl, an integration interval of 9.5-10.4 eV was used (see PES in Fig. 6), and for propyne, the integration interval was 10.2-10.4 eV to discriminate from contributions of allene (see PES in Fig. 8). Compared to the quantitative mole fractions determined with EI-MBMS and VUV-PI-MBMS (Fig. 13), the shape of the profiles and the position of the maxima for both species are in quite satisfactory agreement. Note that an absolute comparison is not intended. The agreement is better between the EI-MBMS and PEPICO experiments because of the identical burner configuration. A shift of the profile for the PI-MBMS experiment to higher HAB is a likely result of the different burner geometries and slightly different flame conditions and was also noted in Ref. 28.

From the fixed-photon-energy measurements performed here, the ratio of the mole fractions for the isomers allene and propyne was also determined and compared with absolute PI-MBMS results. To evaluate this ratio, the spectra of both isomers and the respective photoionisation cross sections must be known. In the measured TPES, contributions from both isomers overlap in the region above 10.2 eV (see Fig. 7); thus the contribution of allene to the propyne signal near its ionisation threshold must be determined independently. In principle this is possible from measured PES; here, however, the fixed photon energies were chosen at a very close distance (at 10.2 and 10.4 eV) and thus did not allow to capture the complete spectrum. We have thus used the literature photoelectron spectra for allene[55] and propyne[56] to simulate the measured TPES point-by-point. In this procedure, the literature spectra were convoluted to provide the same nominal resolution as the measured TPES. The total areas of the literature spectra were integrated in the range of 0-10.9 eV. The sum of the allene and the propyne literature spectrum was then fitted to the experimental TPES using a respective weight factor. The ratio can be described with the following equation:

$$Z = \frac{x_i}{x_j} = f(E) \cdot \frac{\int \sigma_j(E)dE}{\int \sigma_i(E)dE}$$

with *x* being the mole fraction of the respective species i or j, σ the absolute cross sections for the species i or j, *E* the photon energy and *f* the ratio of the signal intensities. For allene and propyne we have chosen the photon energy range of 0-10.9 eV, for which the absolute cross sections measured at 10.9 eV for allene[52] and propyne[52] have been used. Temperature differences between the measured signals and the reference spectra were neglected in a first approximation, assuming limited contribution of this influence in comparison to the overall measurement uncertainties. The resulting relative mole fraction ratio is 3.8±0.8 at the measurement location of the TPES of HAB=4 mm, in very good agreement with the ratio of 3.7 of the maximum absolute mole

fractions determined with PI-MBMS at HAB=3.5 mm.[67] The mole fraction profiles measured with PI-MBMS show different positions of the maxima for allene and propyne, with propyne at 3.25 mm preceding allene at 4 mm. This difference was not resolved in the integrated PES data that were taken with a limited acquisition time of 5 min for each height and a step scan of 0.5 mm.

Similarly to the present example, the method permits in principle to calculate the isomer ratios for *m/z*=54. The mole fraction ratio of 2-butyne/1,3-butadiene determined here is 0.23 at HAB=4 mm and that of 1-butyne/2-butyne at the same position is 6.78. This can be compared to average ratios of 0.24 and 5.79, respectively, determined at HAB=3.5 mm from the absolute mole fractions in the PI-MBMS experiment.[67] While these were in reasonable agreement with the absolute mole fraction ratios determined by PI-MBMS, appropriate selection of the measurement time, height interval and fixed photon energies will be needed to improve the quality of the results. For the evaluation of sets of quantitative mole fractions using the multiplex approach from fixed-photon-energy PEPICO measurements demonstrated here for the first time, care must thus be taken to unambiguously resolve the spectral fingerprints of important species and to provide mass-selected photoelectron spectra at a few but well-chosen photon energies. Furthermore, cross sections for the respective species under study must be known. Here, future applications of the PEPICO technique will be able to profit from the large number of photoionisation cross sections that are already available in the literature. It is also fortuitous that the temperature in the ionisation volume is much lower than that in the flame itself, and close to conditions of literature reference spectra, so that the sensitivity to sampling from different flame locations will be limited and direct simulation of temperature-dependent spectra may not be necessary, at least in a first approximation, for quantitative concentration measurements.

4. Summary and perspectives

Photoelectron-photoion coincidence spectroscopy, a technique which makes use of the information encapsulated in both cations and electrons stemming from the same photoionisation event, had only very recently been applied to analyse complex gas mixtures such as encountered in combustion.[26-28] Up to now, major and intermediate species detection had been demonstrated in the reactive environment of a flame, from spectra obtained by scanning the photon energy in the TPEPICO approach which relies on detection of zero kinetic energy electrons at a given mass.[27,28] For the first time, we have now used fixed-photon-energy PEPICO measurements in a flame using the double-imaging DELICIOUS III spectrometer at the DESIRS beamline of the SOLEIL synchrotron. With a single measurement at a chosen photon energy of 10.2 eV, and a competitive acquisition time of 60 min instead of 30 hours for the corresponding scanning TPEPICO approaches, we could demonstrate in a fuel-rich low-pressure, premixed flat ethene-oxygen-argon flame that multiple intermediate species, including radicals as well as pairs and triplets of isomers, can be unambiguously identified with high reliability. This result was achieved with post-processing the same raw image pair of coincident cations and electrons: key aspects were selecting for different masses and for ions included in the chosen region of interest that corresponds to the central part of the beam, and analysing the mass-filtered electron velocity map images.

Recorded fixed-photon-energy photoelectron spectra were seen to contain distinct fingerprints for the different species and to compare favourably with (scanning) TPES measured in the same flame conditions and literature reference PES for single species. Furthermore, integration of suitable sections of a mass-filtered PI matrix to determine total ion yield was seen to provide excellent agreement with literature photoionisation cross section curves, lending further confidence to the PEPICO technique newly applied under these conditions. While this integration

has been performed to highlight this agreement, it should be kept in mind that PES have an eminent advantage over photoionisation efficiency spectra in that the ionisation threshold can be detected as a clear spike rather than as a change of slope, with the consequent gain in energy precision and contrast.

We have also shown from differentiation of photoionisation cross section curves in recent combustion-relevant compilations[57,64] that superior (fingerprint) structure for individual species in an isomer mix can be obtained even with the fixed-photon-energy approach. The comparison of TPEPICO and PEPICO modes of operation, compared here in a flame for the first time, demonstrates a higher energy resolution for the former – which could be even further increased at the expense of measurement time – and a distinct multiplex advantage for the latter. For potential application of the fixed-photon-energy approach to analyse the flame chemistry, we have shown that mole fraction profiles and isomer ratios can be obtained in good agreement with other photoionisation and electron ionisation molecular-beam mass spectrometry experiments. The temperature in the ionisation region which could be relevant for the quantitative concentration measurements from the PES was analysed and found in good agreement with earlier data from REMPI measurements.[65]

While the first demonstration of the PEPICO technique for multiplexed detections of intermediate species in a flame has only illustrated its potential with a few examples, its use for the analysis of complex reactive mixtures could become similarly widespread as conventional photoionisation mass spectrometry with VUV light from synchrotrons. Decisive advantages of the technique include the availability of fingerprint signatures – the vibrational or electronic structure for the cations – from which unambiguous identification is possible even in situations where onsets from photoionisation efficiency spectra overlap or cannot be measured with sufficient accuracy. For many species, reference spectra are available in the literature; however,

previously undetected species may be encountered in the application of PEPICO spectroscopy to complex reactive environments for which reference spectra must then be obtained from dedicated experiments or theoretical calculations. The time-efficient measurement at a few carefully selected photon energies provides access to numerous chemical species – radical and stable intermediates in the mole fraction ranges of and below 10^{-3} – which can be unambiguously identified, as was demonstrated here from a single recorded PEPICO spectrum at a given photon energy for a mixture of species including a pair and a triplet of isomers at different masses. Such measurements can be performed with high intensity and very good signal to noise, and improvement into the regime of a few ppm seems feasible.

For the development and validation of chemical combustion models, detailed knowledge on the reactive mixture composition is desirable to understand the contributions of pertinent reactions pathways. In this study, isomer separation as well as the determination of their mole fraction ratios was demonstrated. However, for a comprehensive validation, absolute mole fraction of species should be known, and future studies should be focused on the quantification of important combustion species, considering their photoionisation cross sections. For different isomers, their contributions can be determined either from PIE curves or photoelectron spectra. Especially in isomer mixtures of unknown composition, fitting of PIE curves to model different species contributions is error-prone because of unclear ionisation onsets. In such cases, integration of the well-defined PE spectra may significantly improve the isomer-specific quantitative detection. In their recent study, Oßwald et al.[27] have demonstrated improvement of mole fraction determination by PEPICO for the small isomeric molecules acetaldehyde and ethenol. Future work should focus on the quantification of higher molecular species like C5-C7 isomers to further explore the potential and advantages of the PEPICO technique in this context.

The quantification of species usually relies on a mole fraction profile from a reference species such as argon that can be added as an inert gas to the flame. The fixed-photon-energy PEPICO approach demonstrated here can be used to determine quantitative mole fractions from the integrated electron signal similarly to conventional PI-MBMS data evaluation.[68] From the position sensitivity of the ion velocity image, fragmentation can, in principle, be determined, offering another advantage over conventional PI-MBMS. Temperature at the measurement location may need to be determined for quantification, but it is in principle available from the vibrational structure of the PES for species like CH_3, abundant in many flames and thus available as a temperature sensor – again this is information that is not currently available with PI-MBMS. The potential of the approach highlighted here regarding experimental uncertainties in comparison with established laboratory and synchrotron-based MBMS methods will be subject of further studies.

More detailed investigations of flames, with the aim of understanding relevant kinetic mechanisms and pathways as well as using them as convenient species source for spectroscopic studies, are planned on the basis of the present results. In an optimised configuration, a modified burner chamber will reduce the distance between the sampling nozzle and the VUV beam so that further enhancement of signal to noise and thus even faster and/or more precise chemical analysis will become possible.

Acknowledgements

The experiments at SOLEIL were performed under proposal number 20120652. We are grateful to the general SOLEIL staff for running the facility, and to J.-F. Gil for his help in the conception and mounting of the burner chamber and its interface with the SAPHIRS chamber. Partial

support by DFG within SFB 686, TP B3, is gratefully acknowledged. The measurement campaign at the ALS in Berkeley under the direction of Dr. Nils Hansen, with conditions detailed in Ref. 28, from which some selected unpublished results[67] were included in comparison, has involved several members of the "ALS Flame Team" whose contributions to acquiring the data (evaluated by KM and DF) are gratefully acknowledged.

Table 1: Flame conditions for the ϕ=1.7 ethene-oxygen flame stabilized on a 65 mm diameter burner at 40 mbar; all flow rates are given in slm (standard liter per minute at 273.15 K).

C_2H_4 / slm	O_2 / slm	Ar / slm	Total flow / slm	Ar dilution
1.28	2.24	1.17	4.69	25%

Table 2: Species with *m/z*=54 and their ionisation potentials (IPs).

Species	**IP / eV**
1-Butyne	10.18[57]
1,3-Butadiene	9.072±0.007[58]
1,2-Butadiene	9.03[59]
2-Butyne	9.58±0.002[57]

References

1. C. A. Taatjes, D. E. Shallcross and C. J. Percival, *Phys. Chem. Chem. Phys.*, 2014, **16**, 1704–1718.

2. O. Welz, J. D. Savee, D. L. Osborn, S. S. Vasu, C. J. Percival, D. E. Shallcross and C. A. Taatjes, *Science*, 2012, **335**, 204–207.

3. L. Müller, M.-C. Reinnig, K. H. Naumann, H. Saathoff, T. F. Mentel, N. M. Donahue and T. Hoffmann, *Atmos. Chem. Phys.*, 2012, **12**, 1483–1496.

4. M. P. Rissanen, A. J. Eskola, T. L. Nguyen, J. R. Barker, J. Liu, J. Liu, E. Halme and R. S. Timonen, *J. Phys. Chem. A*, 2014, **118**, 2176–2186.

5. J. Zádor, H. Huang, O. Welz, J. Zetterberg, D. L. Osborn and C. A. Taatjes, *Phys. Chem. Chem. Phys.*, 2013, **15**, 10753–10760.

6. O. Herbinet, F. Battin-Leclerc, S. Bax, H. Le Gall, P.-A. Glaude, R. Fournet, Z. Zhou, L. Deng, H. Guo, M. Xie and F. Qi, *Phys. Chem. Chem. Phys.*, 2011, **13**, 296–308.

7. N. Hansen, M. R. Harper and W. H. Green, *Phys. Chem. Chem. Phys.*, 2011, **13**, 20262–20274.

8. K. Kohse-Höinghaus, P. Oßwald, T. A. Cool, T. Kasper, N. Hansen, F. Qi, C. K. Westbrook and P. R. Westmoreland, *Angew. Chem. Int. Ed.*, 2010, **49**, 3572–3597.

9. D. S. N. Parker, F. Zhang, Y. S. Kim, R. I. Kaiser, A. Landera, V. V Kislov, A. M. Mebel and A. G. G. M. Tielens, *Proc. Natl. Acad. Sci.*, 2012, **109**, 53–58.

10. B. B. Dangi, S. Maity, R. I. Kaiser and A. M. Mebel, *J. Phys. Chem. A*, 2013, **117**, 11783–11793.

11. M. W. Kelly, J. C. Richley, C. M. Western, M. N. R. Ashfold and Y. A. Mankelevich, *J. Phys. Chem. A*, 2012, **116**, 9431–9446.

12. K. Kohse-Höinghaus, R. S. Barlow, M. Aldén and J. Wolfrum, *Proc. Combust. Inst.*, 2005, **30**, 89–123.

13. R. K. Hanson, *Proc. Combust. Inst.*, 2011, **33**, 1–40.

14. R. S. Barlow, G.-H. Wang, P. Anselmo-Filho, M. S. Sweeney and S. Hochgreb, *Proc. Combust. Inst.*, 2009, **32**, 945–953.

15. D. S. Baer, R. K. Hanson, M. E. Newfield and N. K. J. M. Gopaul, *Opt. Lett.*, 1994, **19**, 1900–1902.

16. J. H. Northern, A. W. J. Thompson, M. L. Hamilton and P. Ewart, *Appl. Phys. B*, 2013, **111**, 627–635.

17. N. Hansen, T. A. Cool, P. R. Westmoreland and K. Kohse-Höinghaus, *Prog. Energy Combust. Sci.*, 2009, **35**, 168–191.

18. T. A. Cool, A. McIlroy, F. Qi, P. R. Westmoreland, L. Poisson, D. S. Peterka and M. Ahmed, *Rev. Sci. Instrum.*, 2005, **76**, 094102.

19. Y. Li and F. Qi, *Acc. Chem. Res.*, 2010, **43**, 68–78.

20. J. Wang, M. Chaos, B. Yang, T. A. Cool, F. L. Dryer, T. Kasper, N. Hansen, P. Oßwald, K. Kohse-Höinghaus and P. R. Westmoreland, *Phys. Chem. Chem. Phys.*, 2009, **11**, 1328–1339.

21. C. A. Taatjes, N. Hansen, A. McIlroy, J. A. Miller, J. P. Senosiain, S. J. Klippenstein, F. Qi, L. Sheng, Y. Zhang, T. A. Cool, J. Wang, P. R. Westmoreland, M. E. Law, T. Kasper and K. Kohse-Höinghaus, *Science*, 2005, **308**, 1887–1889.

22. S. R. Leone, M. Ahmed and K. R. Wilson, *Phys. Chem. Chem. Phys.*, 2010, **12,** 6564–6578.

23. B. Yang, P. Oßwald, Y. Li, J. Wang, L. Wei, Z. Tian, F. Qi and K. Kohse-Höinghaus, *Combust. Flame*, 2007, **148**, 198–209.

24. J. D. Savee, O. Welz, C. A. Taatjes and D. L. Osborn, *Phys. Chem. Chem. Phys.*, 2012, **14**, 10410–10423.

25. C. A. Taatjes, N. Hansen, D. L. Osborn, K. Kohse-Höinghaus, T. A. Cool and P. R. Westmoreland, *Phys. Chem. Chem. Phys.*, 2008, **10**, 20–34.

26. A. Bodi, P. Hemberger, D. L. Osborn and B. Sztáray, *J. Phys. Chem. Lett.*, 2013, **4**, 2948–2952.

27. P. Oßwald, P. Hemberger, T. Bierkandt, E. Akyildiz, M. Köhler, A. Bodi, T. Gerber and T. Kasper, *Rev. Sci. Instrum.*, 2014, **85**, 025101.

28. D. Felsmann, K. Moshammer, J. Krüger, A. Lackner, A. Brockhinke, T. Kasper, T. Bierkandt, E. Akyildiz, N. Hansen, A. Lucassen, P. Oßwald, M. Köhler, G. A. Garcia, L. Nahon, P. Hemberger, A. Bodi, T. Gerber and K. Kohse-Höinghaus, *Proc. Combust. Inst.*, 2015, **35**, DOI: 10.1016/j.proci.2014.05.151.

29. C. J. Danby and H. D. Eland, *Int. J. Mass Spectrom. Ion Phys.*, 1972, **8**, 153–161.

30. B. Brehm, J. H. D. Elland, R. Frey and A. Küstler, *Int. J. Mass Spectrom. Ion Phys.*, 1973, **12**, 213–224.

31. T. Baer and Y. Li, *Int. J. Mass Spectrom.*, 2002, **219**, 381–389.

32. B. Sztáray and T. Baer, *Rev. Sci. Instrum.*, 2003, **74**, 3763–3768.

33. A. Bodi, M. Johnson, T. Gerber, Z. Gengeliczki, B. Sztáray and T. Baer, *Rev. Sci. Instrum.*, 2009, **80**, 034101.

34. G. A. Garcia, H. Soldi-Lose and L. Nahon, *Rev. Sci. Instrum.*, 2009, **80**, 023102.

35. G. A. Garcia, B. K. Cunha de Miranda, M. Tia, S. Daly and L. Nahon, *Rev. Sci. Instrum.*, 2013, **84**, 053112.

36. H. M. Rosenstock, K. Draxl, B. W. Steiner and J. T. Herron, *NIST Chemistry WebBook, NIST Standard Reference Database Number 69*, P. J. Linstrom and W. G. Mallard (Eds.), National Institute of Standards and Technology, Gaithersburg MD, 20899, http://webbook.nist.gov (retrieved August 20, 2014).

37. T. Baer and P. M. Guyon, *An historical introduction to threshold photoionization*, in *High resolution laser photoionization and photoelectron studies*, ed. I. Powis, T. Baer and C.-Y. Ng, John Wiley & Sons, Chichester, 1995, pp. 1–16.

38. A. Bodi, P. Hemberger, T. Gerber and B. Sztáray, *Rev. Sci. Instrum.*, 2012, **83**, 083105.

39. M. Steinbauer, P. Hemberger, I. Fischer and A. Bodi, *ChemPhysChem*, 2011, **12**, 1795–1797.

40. P. Hemberger, M. Steinbauer, M. Schneider, I. Fischer, M. Johnson, A. Bodi and T. Gerber, *J. Phys. Chem. A*, 2010, **114**, 4698–4703.

41. P. Hemberger, M. Lang, B. Noller, I. Fischer, C. Alcaraz, B. K. Cunha de Miranda, G. A. Garcia and H. Soldi-Lose, *J. Phys. Chem. A*, 2011, **115**, 2225–2230.

42. H. Dossmann, G. A. Garcia, L. Nahon, B. K. C. de Miranda and C. Alcaraz, *J. Chem. Phys.*, 2012, **136**, 204304.

43. D. Baker, D. Betteridge, N. R. Kemp and R. E. Kirby, *Anal. Chem.*, 1970, **42**, 1064-1073.

44. G. Martins, A. M. Ferreira-Rodrigues, F. N. Rodrigues, G. G. B. de Souza, N. J. Mason, S. Eden, D. Duflot, J.-P. Flament, S. V. Hoffmann, J. Delwiche, M.-J. Hubin-Franskin and P. Limão-Vieira, *Phys. Chem. Chem. Phys*, 2009, **11**, 11219-11231.

45. L. Nahon, N. de Oliveira, G. A. Garcia, J. F. Gil, B. Pilette, O. Marcouille, B. Lagarde and F. Polack, *J. Synchrotron Rad.,* 2012, **19**, 508–520.

46. G. A. Garcia, L. Nahon and I. Powis, *Rev. Sci. Instrum.*, 2004, **75**, 4989–4996.

47. J. C. Poully, J. P. Schermann, N. Nieuwjaer, F. Lecomte, G. Grégoire, C. Desfrançois, G. A. Garcia, L. Nahon, D. Nandi, L. Poisson and M. Hochlaf, *Phys. Chem. Chem. Phys.*, 2010, **12**, 3566–3572.

48. M. Schenk, L. Leon, K. Moshammer, P. Oßwald, T. Zeuch, L. Seidel, F. Mauss and K. Kohse-Höinghaus, *Combust. Flame*, 2013, **160**, 487–503.

49. P. Oßwald, K. Kohse-Höinghaus, U. Struckmeier, T. Zeuch, L. Seidel, L. Leon and F. Mauss, *Z. Phys. Chem.*, 2011, **225**, 1029–1054.

50. J. D. Savee, S. Soorkia, O. Welz, T. M. Selby, C. A. Taatjes and D. L. Osborn, *J. Chem. Phys.*, 2012, **136**, 134307.

51. B. K. Cunha de Miranda, C. Alcaraz, M. Elhanine, B. Noller, P. Hemberger, I. Fischer, G. A. Garcia, H. Soldi-Lose, B. Gans, L. A. Vieira Mendes, S. Boyé-Péronne, S. Douin, J. Zabka and P. Botschwina, *J. Phys. Chem. A*, 2010, **114**, 4818–4830.

52. T. A. Cool, K. Nakajima, T. A. Mostefaoui, F. Qi, A. McIlroy, P. R. Westmoreland, M. E. Law, L. Poisson, D. S. Peterka and M. Ahmed, *J. Chem. Phys.*, 2003, **119**, 8356–8365.

53. R. Stockbauer, K. E. McCulloh and A. C. Parr, *Int. J. Mass Spectrom. Ion Phys.*, 1979, **31**, 187–189.

54. A. C. Parr, A. J. Jason, R. Stockbauer and K. E. McCulloh, *Int. J. Mass Spectrom. Ion Phys.*, 1979, **30**, 319–330.

55. Z. Z. Yang, L. S. Wang, Y. T. Lee, D. A. Shirley, S. Y. Huang and W. A. Lester Jr, *Chem. Phys. Lett.*, 1990, **171**, 9–13.

56. P. Carlier, J. E. Dubois, P. Masclet and G. Mouvier, *J. Electron Spectros. Relat. Phenomena*, 1975, **7**, 55–67.

57. J. Wang, B. Yang, T. A. Cool, N. Hansen and T. Kasper, *Int. J. Mass Spectrom.*, 2008, **269**, 210–220.

58. T. A. Cool, J. Wang, K. Nakajima, C. A. Taatjes and A. McIlroy, *Int. J. Mass Spectrom.*, 2005, **247**, 18–27.

59. M. Beez, G. Bieri, H. Bock and E. Heilbronner, *Helv. Chim. Acta*, 1973, **56**, 1028–1046.

60. N. Hansen, T. Kasper, S. J. Klippenstein, P. R. Westmoreland, M. E. Law, C. A. Taatjes, K. Kohse-Höinghaus, J. Wang and T. A. Cool, *J. Phys. Chem. A*, 2007, **111**, 4081–4092.

61. P. Oßwald, H. Güldenberg, K. Kohse-Höinghaus, B. Yang, T. Yuan and F. Qi, *Combust. Flame*, 2011, **158**, 2–15.

62. D. M. P. Holland, M. A. MacDonald, M. A. Hayes, P. Baltzer, B. Wannberg, M. Lundqvist, L. Karlsson and W. von Niessen, *J. Phys. B: At. Mol. Opt. Phys.*, 1996, **29**, 3091–3107.

63. A. S. Werner and T. Baer, *J. Chem. Phys.*, 1975, **62**, 2900–2910.

64. B. Yang, J. Wang, T. A. Cool, N. Hansen, S. Skeen and D. L. Osborn, *Int. J. Mass Spectrom.*, 2012, **309**, 118–128.

65. M. Kamphus, N.-N. Liu, B. Atakan, F. Qi and A. McIlroy, *Proc. Combust. Inst.*, 2002, **29**, 2627–2633.

66. C. A. Taatjes, N. Hansen, J. A. Miller, T. A. Cool, J. Wang, P. R. Westmoreland, M. E. Law, T. Kasper and K. Kohse-Höinghaus, *J. Chem. Phys. A*, 2006, **110**, 3254–3260.

67. T. Bierkandt, D. Felsmann, N. Hansen and K. Moshammer, unpublished EI-MBMS and PI-MBMS results for the flame conditions (and taken as part of the same set of experiments), reported in Ref. 27.

68. T. Kasper, P. Oßwald, U. Struckmeier, K. Kohse-Höinghaus, C.A. Taatjes, J. Wang, T.A. Cool, M. E. Law, A. Morel and P. R. Westmoreland, *Combust. Flame*, 2009, **156**,1181-1201.

Figure captions

Figure 1: PEPICO flame experiment at SOLEIL; left: 3D rendering, right: schematic set-up. Gas samples are extracted from the flame with a quartz nozzle and expanded into the ionisation chamber at the SAPHIRS endstation. Molecules are photoionised by the VUV synchrotron radiation of the DESIRS beamline. Ions (M^+) and electrons (e^-) are detected in coincidence by the DELICIOUS III spectrometer.

Figure 2: a) Filtered time-of-flight mass spectrum (upper trace) for ions in the region of interest (ROI) highlighted in b) as well as the unfiltered time-of-flight mass spectrum (lower trace) recorded in the ϕ=1.7 ethene-oxygen flame at HAB=4 mm at 10.2 eV, showing signatures of a number of combustion intermediates. Raw ion (b) and electron (c) images, corresponding to all masses, detected under the same conditions as mentioned above. The elongated shape of the image is due to the large ionisation volume. d) Filtered electron image for coincident ions located in the ROI. The colour code for images b)-d) is shown on the right of panel b).

Figure 3: Top: PI matrix for *m/z*=15 representing the kinetic energy of the electrons (Ele KE) as a function of photon energy. Bottom: threshold photoelectron spectrum (TPES) and total ion yield (TIY) evaluated from the PI matrix, compared with literature photoionisation cross section (PICS) at *m/z*=15 (corresponding to the methyl radical).[50] The acquisition time was 30 hours.

Figure 4: Velocity map image (VMI) obtained at hν=10.2 eV in the ϕ=1.7 ethene-oxygen flame at HAB=4 mm, mass-selected for *m/z*=15 (methyl radical, CH_3). The image is split to show the signal before (left) and after (right) treatment of the raw data with the pBasex Abel inversion algorithm.[46] The acquisition time was 60 minutes. In addition the corresponding PES for *m*/*z*=15 is shown in the right part of Fig. 4.

Figure 5: Literature photoionisation cross sections (PICS) for allene and propyne at *m/z*=44[52] and total ion yield (TIY) at *m/z*=40 from this work. The ionisation energies of 9.691±0.003 eV for allene[53] and 10.37±0.01 eV for propyne[54] are marked by the arrows. The weighted sum of the cross sections obtained with the relative amounts of the two isomers determined in the flame is included for comparison.

Figure 6: Comparison of measured TPES (30 hours acquisition) and PES (1 hour acquisition) at a fixed photon energy of 10.2 eV in the ϕ=1.7 ethene-oxygen flame at HAB=4 mm with reference TPES from the literature.[51]

Figure 7: TPES with photon energy scanned from 9 to 12 eV, filtered for mass 40. Allene and propyne are identified compared to literature PES of allene[55] and propyne.[56] The insert highlights the allene fingerprint region; the measured spectrum was multiplied by a factor of 34 for clarity.

Figure 8: Left: PES for *m/z*=40 recorded at fixed photon energy of 10.4 eV compared with TPES (see Fig. 9). The insert highlights the allene fingerprint region; the measured spectrum was multiplied by a factor of 31 for clarity. Right: Comparison of the PES recorded at fixed photon energy of 10.2 eV with the TPES literature spectrum of allene.[55]

Figure 9: TPES for *m/z*=54 recorded in the photon energy range of 9-12 eV, compared with literature PES for the isomers 1,3-butadiene,[62] 2-butyne[56] and 1-butyne.[63]

Figure 10: Comparison for *m/z*=54 of TPES recorded in the photon energy range of 9-12 eV with PES at fixed photon energy of 10.2 eV.

Figure 11: Spectra obtained for *m/z*=54 in the ϕ=1.7 ethene-oxygen flame at HAB=4 mm. Left: spectra for 1,3-butadiene including TPES from this work, derivative of photoionisation cross section reported by Yang et al.[64] and reference PES of 1,3-butadiene.[62] Right: spectra for

2-butyne including TPES and PES at 10.2 eV measured here, derivative of cross section given by Wang et al.[57] and reference PES of 2-butyne.[56]

Figure 12: Mass-selected threshold photoelectron spectrum for *m/z*=15. The calculated stick spectrum (red) represents a temperature of 280 K, compared with that of 550 K (blue) from a flash pyrolysis experiment.[51]

Figure 13: Species profiles for methyl (left) and propyne (right) as obtained by integration of PES recorded at a single photon energy of 10.4 eV. For comparison, absolute mole fraction profiles are included that have been determined by EI-MBMS and PI-MBMS.[67]

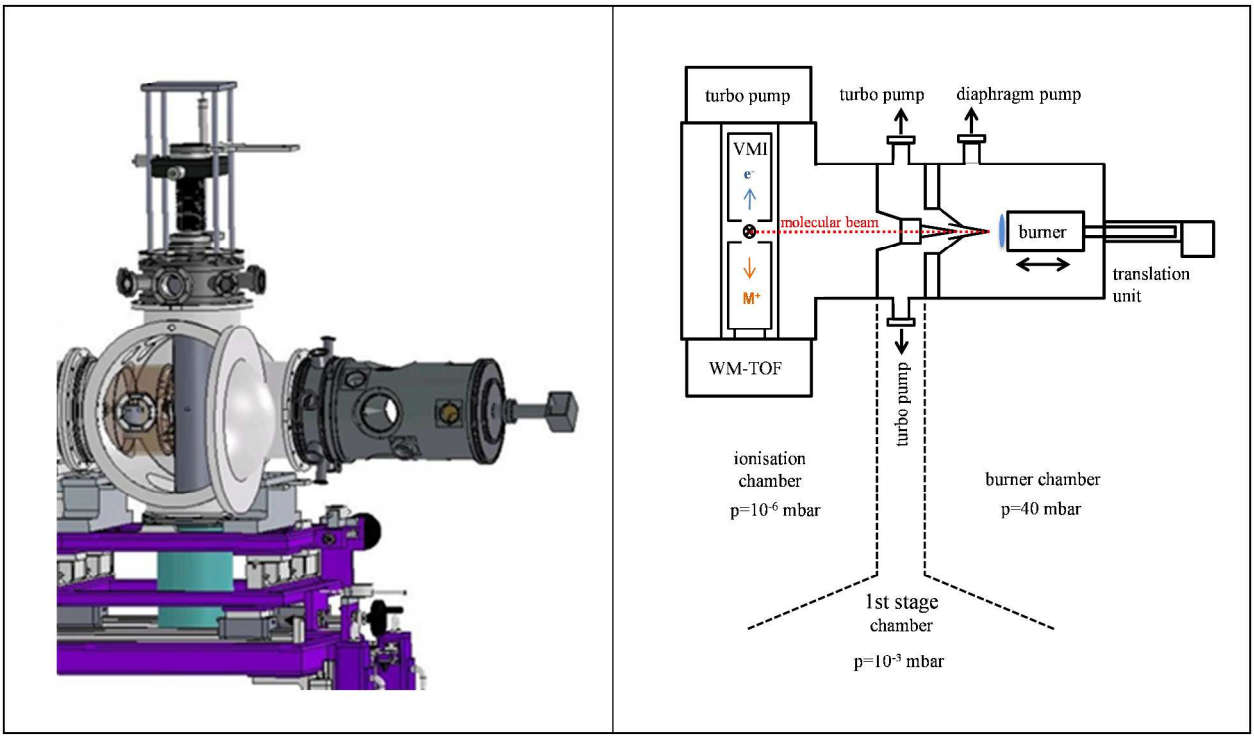

Figure 1: PEPICO flame experiment at SOLEIL; left: 3D rendering, right: schematic set-up. Gas samples are extracted from the flame with a quartz nozzle and expanded into the ionisation chamber at the SAPHIRS endstation. Molecules are photoionised by the VUV synchrotron radiation of the DESIRS beamline. Ions (M^+) and electrons (e^-) are detected in coincidence by the DELICIOUS III spectrometer.

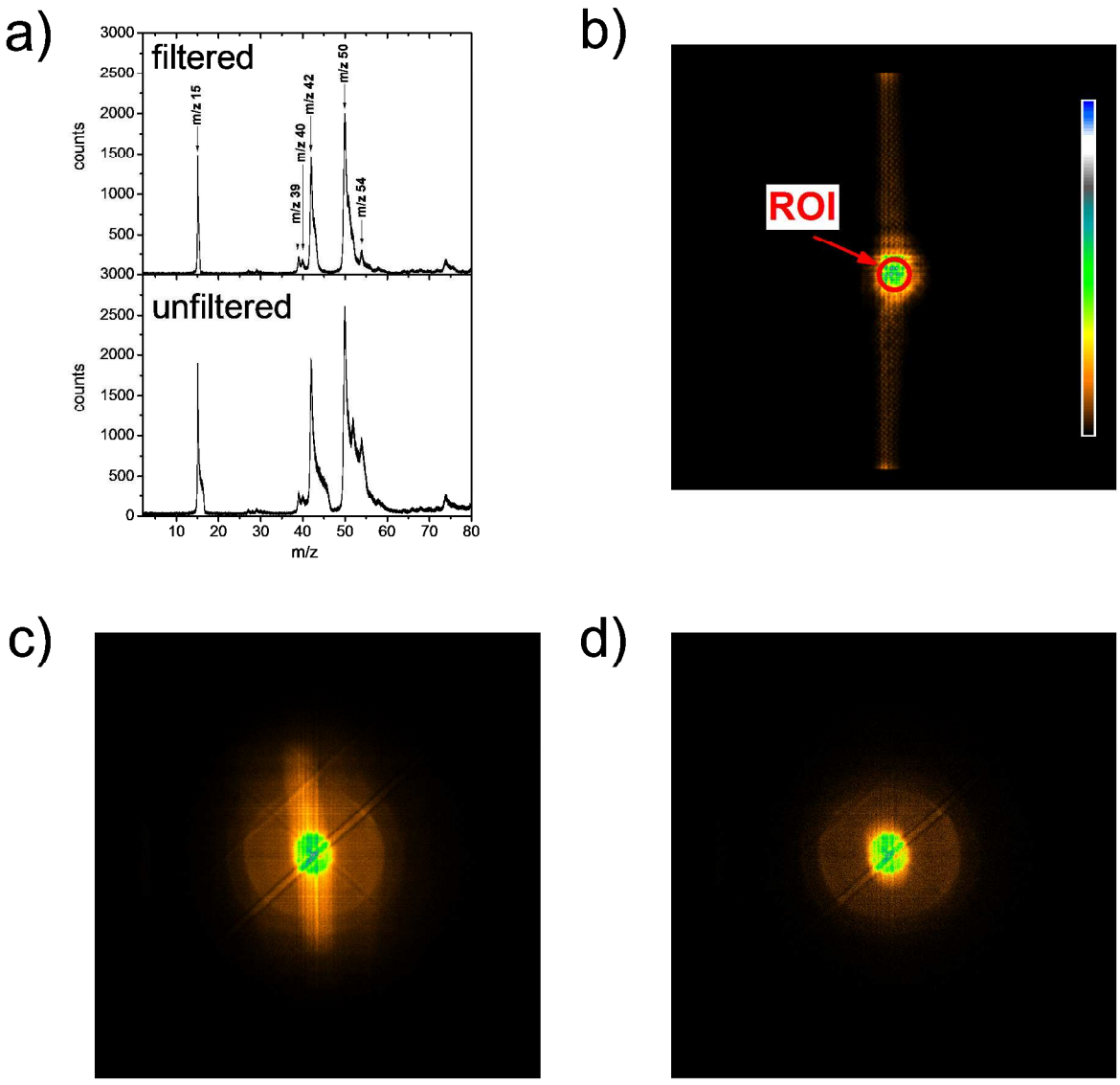

Figure 2: a) Filtered time-of-flight mass spectrum (upper trace) for ions in the region of interest (ROI) highlighted in b) as well as the unfiltered time-of-flight mass spectrum (lower trace) recorded in the ϕ=1.7 ethene-oxygen flame at HAB=4 mm at 10.2 eV, showing signatures of a number of combustion intermediates. Raw ion (b) and electron (c) images, corresponding to all masses, detected under the same conditions as mentioned above. The elongated shape of the image is due to the large ionisation volume. d) Filtered electron image for coincident ions located in the ROI. The colour code for images b)-d) is shown on the right of panel b).

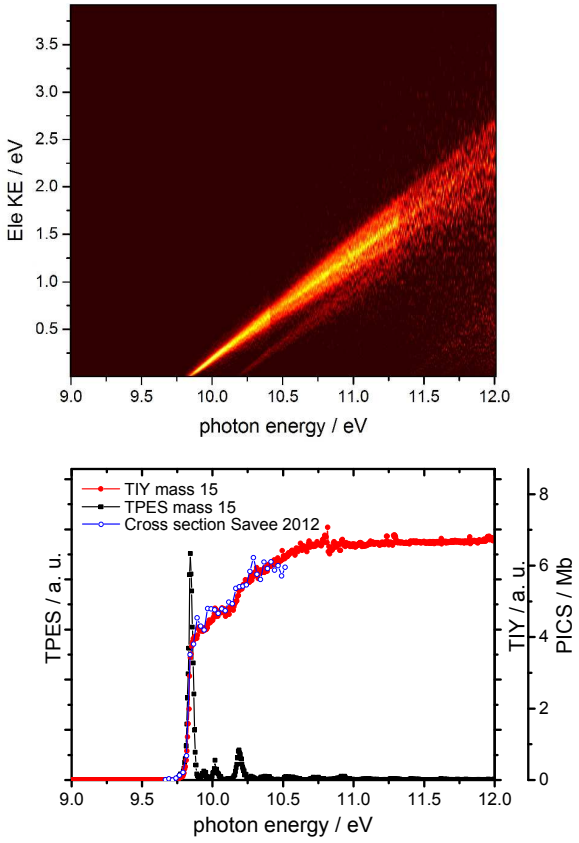

Figure 3: Top: PI matrix for *m/z*=15 representing the kinetic energy of the electrons (Ele KE) as a function of photon energy. Bottom: threshold photoelectron spectrum (TPES) and total ion yield (TIY) evaluated from the PI matrix, compared with literature photoionisation cross section (PICS) at *m/z*=15 (corresponding to the methyl radical).[50] The acquisition time was 30 hours.

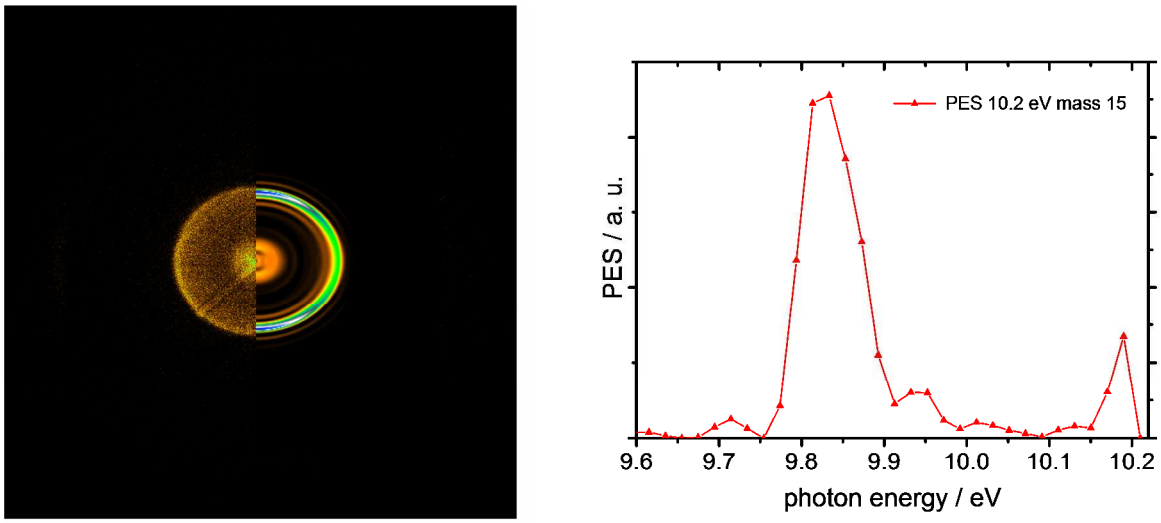

Figure 4: Velocity map image (VMI) obtained at hν=10.2 eV in the ϕ=1.7 ethene-oxygen flame at HAB=4 mm, mass-selected for *m/z*=15 (methyl radical, CH_3). The image is split to show the signal before (left) and after (right) treatment of the raw data with the pBasex Abel inversion algorithm.[46] The acquisition time was 60 minutes. In addition the corresponding PES for *m/z*=15 is shown in the right part of Fig. 4.

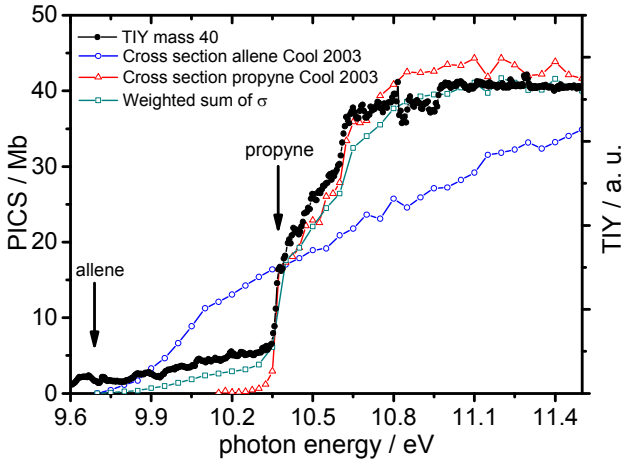

Figure 5: Literature photoionisation cross sections (PICS) for allene and propyne at *m/z*=44[52] and total ion yield (TIY) at *m/z*=40 from this work. The ionisation energies of 9.691±0.003 eV for allene[53] and 10.37±0.01 eV for propyne[54] are marked by the arrows. The weighted sum of the cross sections obtained with the relative amounts of the two isomers determined in the flame is included for comparison.

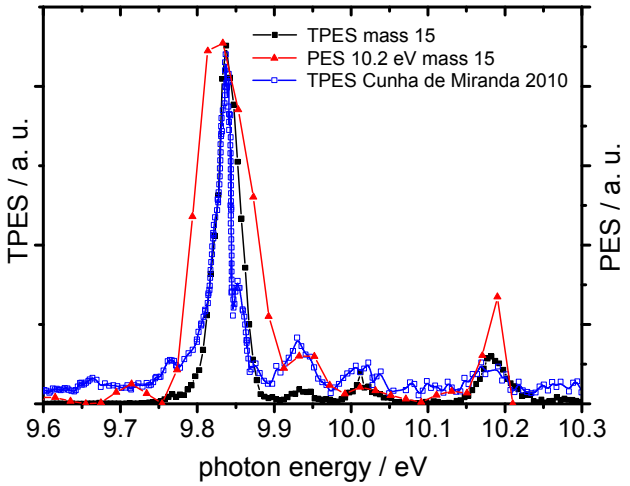

Figure 6: Comparison of measured TPES (30 hours acquisition) and PES (1 hour acquisition) at a fixed photon energy of 10.2 eV in the ϕ=1.7 ethene-oxygen flame at HAB=4 mm with reference TPES from the literature.[51]

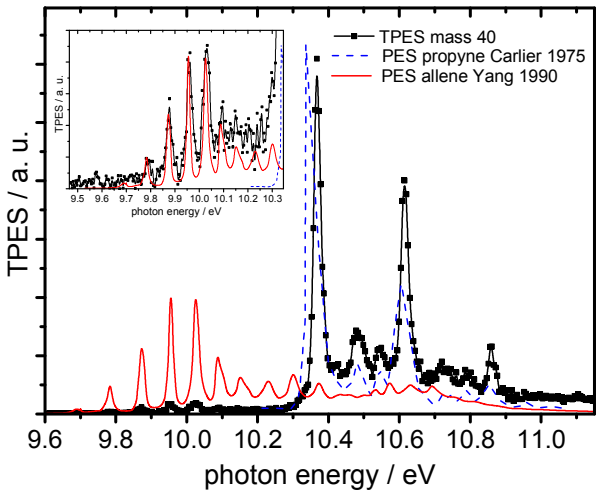

Figure 7: TPES with photon energy scanned from 9 to 12 eV, filtered for mass 40. Allene and propyne are identified compared to literature PES of allene[55] and propyne.[56] The insert highlights the allene fingerprint region; the measured spectrum was multiplied by a factor of 34 for clarity.

.

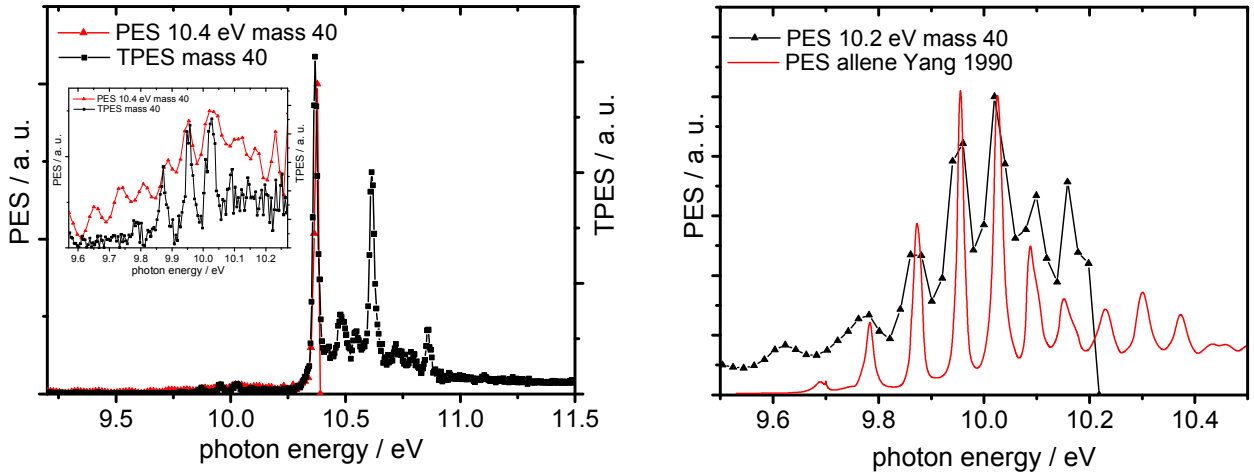

Figure 8: Left: PES for *m/z*=40 recorded at fixed photon energy of 10.4 eV compared with TPES (see Fig. 9). The insert highlights the allene fingerprint region; the measured spectrum was multiplied by a factor of 31 for clarity. Right: Comparison of the PES recorded at fixed photon energy of 10.2 eV with the TPES literature spectrum of allene.[55]

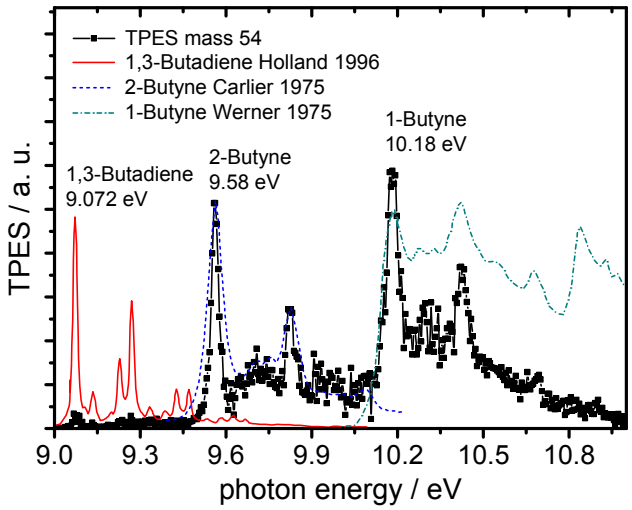

Figure 9: TPES for *m/z*=54 recorded in the photon energy range of 9-12 eV, compared with literature PES for the isomers 1,3-butadiene,[62] 2-butyne[56] and 1-butyne.[63]

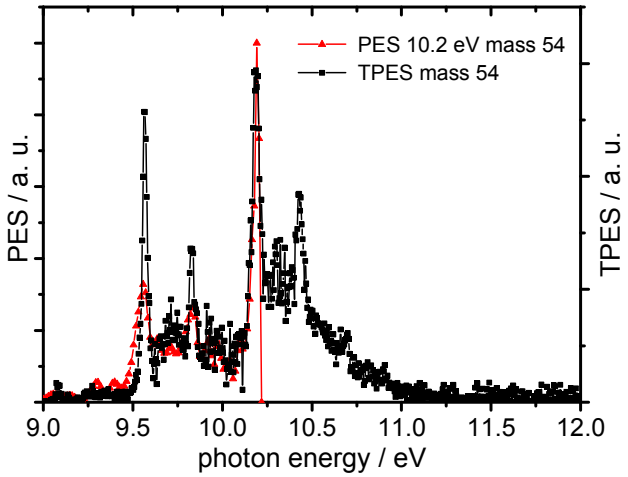

Figure 10: Comparison for *m/z*=54 of TPES recorded in the photon energy range of 9-12 eV with PES at fixed photon energy of 10.2 eV.

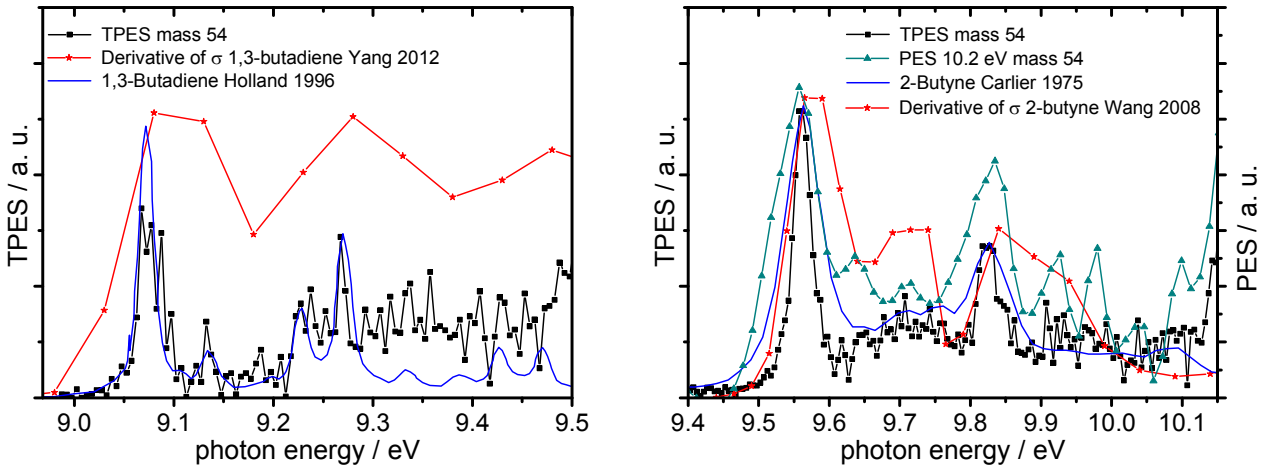

Figure 11: Spectra obtained for *m/z*=54 in the ϕ=1.7 ethene-oxygen flame at HAB=4 mm. Left: spectra for 1,3-butadiene including TPES from this work, derivative of photoionisation cross section reported by Yang et al.[64] and reference PES of 1,3-butadiene.[62] Right: spectra for 2-butyne including TPES and PES at 10.2 eV measured here, derivative of cross section given by Wang et al.[57] and reference PES of 2-butyne.[56]

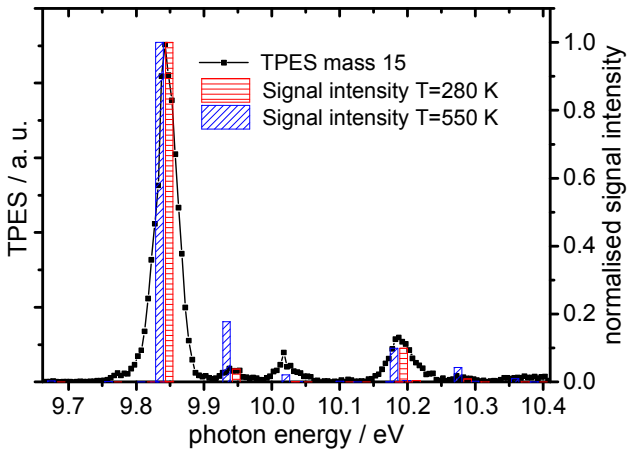

Figure 12: Mass-selected threshold photoelectron spectrum for *m/z*=15. The calculated stick spectrum (red) represents a temperature of 280 K, compared with that of 550 K (blue) from a flash pyrolysis experiment.[51]

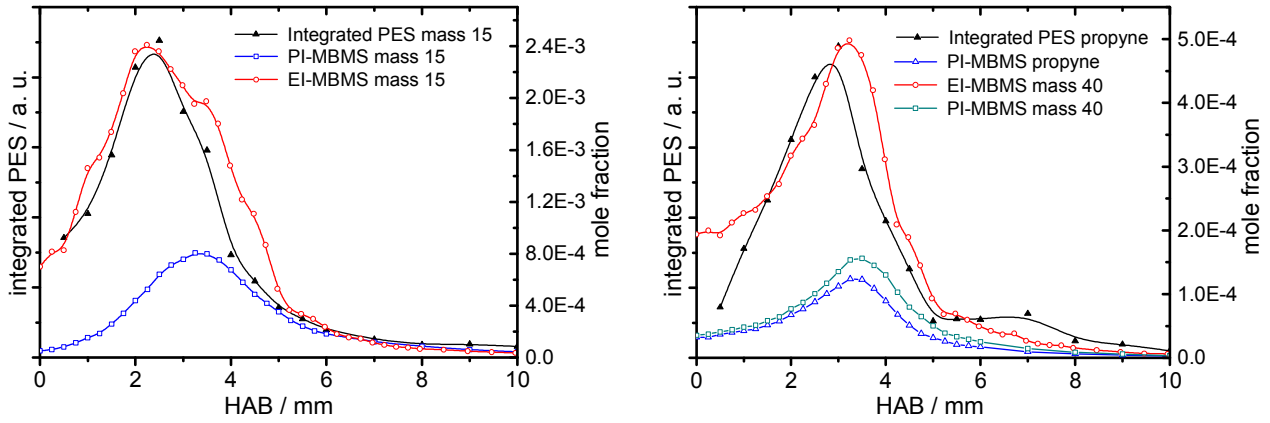

Figure 13: Species profiles for methyl (left) and propyne (right) as obtained by integration of PES recorded at a single photon energy of 10.4 eV. For comparison, absolute mole fraction profiles are included that have been determined by EI-MBMS and PI-MBMS.[67]